

PAPER

Visible to near-infrared photodetectors based on MoS₂ vertical Schottky junctions



To cite this article: Fan Gong *et al* 2017 *Nanotechnology* **28** 484002

View the [article online](#) for updates and enhancements.

Related content

- [Photodetecting and light-emitting devices based on two-dimensional materials](#)
Yuanfang Yu, Feng Miao, Jun He et al.
- [Air-stable few-layer black phosphorus phototransistor for near-infrared detection](#)
Junhong Na, Kichul Park, Jin Tae Kim et al.
- [Highly Efficient, High Speed Vertical Photodiodes based on Few-layer MoS₂](#)
Zhen Li, Jihan Chen, Rohan Dhall et al.

Visible to near-infrared photodetectors based on MoS₂ vertical Schottky junctions

Fan Gong^{1,2,3,6}, Hehai Fang^{2,3,6}, Peng Wang^{2,3}, Meng Su¹, Qing Li², Johnny C Ho⁴ , Xiaoshuang Chen^{2,3}, Wei Lu^{2,3}, Lei Liao¹, Jun Wang^{5,7} and Weida Hu^{2,7} 

¹ Department of Physics and Key Laboratory of Artificial Micro- and Nano-structures of Ministry of Education, Wuhan University, Wuhan 430072, People's Republic of China

² State Key Laboratory of Infrared Physics, Shanghai Institute of Technical Physics, Chinese Academy of Sciences, Shanghai 200083, People's Republic of China

³ Synergetic Innovation Center of Quantum Information and Quantum Physics, University of Science and Technology of China, Hefei 230026, People's Republic of China

⁴ Department of Materials Science and Engineering, City University of Hong Kong, Hong Kong SAR, People's Republic of China

⁵ School of Optoelectronic Information, State Key Laboratory of Electronic Thin Films and Integrated Devices, University of Electronic Science and Technology of China, Chengdu 610054, People's Republic of China

E-mail: wjun@uestc.edu.cn and wdhu@mail.sitp.ac.cn

Received 18 July 2017, revised 4 September 2017

Accepted for publication 5 October 2017

Published 9 November 2017



CrossMark

Abstract

Over the past few years, two-dimensional (2D) nanomaterials, such as MoS₂, have been widely considered as the promising channel materials for next-generation high-performance phototransistors. However, their device performances still mostly suffer from slow photoresponse (e.g. with the time constant in the order of milliseconds) due to the relatively long channel length and the substantial surface defect induced carrier trapping, as well as the insufficient detectivity owing to the relatively large dark current. In this work, a simple multilayer MoS₂ based photodetector employing vertical Schottky junctions of Au-MoS₂-ITO is demonstrated. This unique device structure can significantly suppress the dark current down to 10⁻¹² A and enable the fast photoresponse of 64 μs, together with the stable responsivity of ~1 A W⁻¹ and the high photocurrent to dark current ratio of ~10⁶ at room temperature. This vertical-Schottky photodetector can also exhibit a wide detection range from visible to 1000 nm. All these results demonstrate clearly that the vertical Schottky structure is an effective configuration for achieving high-performance optoelectronic devices based on 2D materials.

Supplementary material for this article is available [online](#)

Keywords: MoS₂, vertical Schottky junction, dark current, photodetectors

(Some figures may appear in colour only in the online journal)

1. Introduction

In recent years, due to the unique properties, a wide variety of two-dimensional (2D) materials and their heterostructures have been widely studied as promising active materials

for next-generation electronics. However, since the high ON/OFF current ratio is essential for high-performance electronic and optoelectronic devices, graphene, the typical 2D material, has the zero band gap and significant leakage current, in which all these would restrict its utilization in those application domains [1]. As compared with graphene, MoS₂, made up of layered S–Mo–S atoms bonded by weak van der Waals forces, is another semiconducting 2D material with a

⁶ These authors contributed equally to this work.

⁷ Authors to whom any correspondence should be addressed.

much larger bandgap of ~ 1.8 eV. Generally, when MoS₂ is thinned down to the 2D monolayer, the broken inversion symmetry and indirect-to-direct bandgap transition are correspondingly observed as a result of quantum confinement [2–4]. Also, the mechanical strength of MoS₂ membrane is 30 times higher than that of steel while the stability can be maintained up to 1100 °C in an inert environment [5]. When fabricated into field-effect transistors, these monolayer or few-layer based devices exhibit a high ON/OFF current ratio of 10^7 , an impressive drain current density of $240 \mu\text{A} \mu\text{m}^{-1}$ and a peak field-effect mobility of $184 \text{cm}^2 \text{V}^{-1} \text{s}^{-1}$ [6]. In this regard, MoS₂ has become an ideal candidate of channel materials among many 2D materials for various applications.

In specific, Yin *et al* reported monolayer MoS₂ based photodetectors, demonstrating a photoresponsivity of 7.5mA W^{-1} when the illumination power, bias and gate voltages are $80 \mu\text{W}$, 1 V and 50 V, respectively [7]. Although these photodetectors can outperform the single-layer graphene based photodetectors in terms of the responsivity by almost ten times [1, 8], the response time (i.e. 50 ms) of MoS₂ based detectors is not quite as fast as the one of graphene counterparts [7]. Recently, high-performance MoS₂ photodetectors have been achieved utilizing unique device structures and/or special designs. The highest responsivity of MoS₂ photodetectors can reach 880A W^{-1} under an ultralow illumination power of 150 pW (i.e. 24W cm^{-2}) when a substantially high back-gate voltage of 70 V and a large drain bias of 8 V is applied [9]. Despite the high responsivity, this type of photodetectors still display an insufficient response with the long rise time (t_{rise}) and inefficient decay time (t_{decay}) of 4 s and 9 s, accordingly. This relatively slow response is attributed to the trap states existed on the MoS₂ device channel surface and/or located at the interface between MoS₂ channel and underlying SiO₂ dielectric layer, which capture photo-generated electrons and then result in the long lifetimes of photo-generated holes. Hence, these devices sacrifice their photoresponse speed in order to obtain the high photoresponse gain [10]. In addition, the responsivity of monolayer MoS₂ based photodetectors can be further increased by decreasing the illumination laser power, in which this enhancement can be partly owing to the absorption saturation in MoS₂ and partly in consequence of the screening of a built-in electric field caused by the photoexcited electrons in the conduction band of MoS₂ [11]. At the same time, the MoS₂ device can be integrated with a ferroelectric polymer film to exhibit a maximum responsivity of 2570A W^{-1} under a low illumination power of 1 nW at a zero gate voltage and a V_{ds} of 5 V [12]. It is noted that this ferroelectric polymer film plays a crucial role to strongly suppress the dark current and help to realize a highly sensitive photodetector. More importantly, the t_{rise} and t_{decay} of such device are observed to be 1.8 ms and 2.0 ms, respectively, which are much faster than those of state-of-the-art MoS₂ based photoconductive devices. In any case, to the best of our knowledge, the photoresponse time of most MoS₂ devices is yet limited in the order of milliseconds.

With the purpose to further optimize these figures of merit, in this work, we design and fabricate multilayer MoS₂ based photodetectors employing simple vertical Schottky junctions of gold-MoS₂-indium tin oxide (Au-MoS₂-ITO). Impressively, the obtained device exhibits the excellent

detector performance with a fast response time of $64 \mu\text{s}$, a stable responsivity of $\sim 1 \text{A W}^{-1}$, a high photocurrent to dark current ratio of 10^6 and an ultralow dark current of 10^{-12}A at a zero bias in ambient environment. This superior photoresponse is ascribed to the extremely short channel length configured in the vertical manner for the fast transit time as well as the built-in electric field associated to accelerate the separation of photogenerated electron-hole pairs. All these results evidently indicate the technological potency of vertical Schottky structure as an effective configuration for achieving high-performance optoelectronic devices.

2. Experiment

2.1. Fabrication of photodetectors

The multilayer MoS₂ was mechanically exfoliated from commercially available crystals (purchased from SPI supplies). The layers were distinguished by the observation under optical microscopy and Raman spectroscopy on a 300 nm thick SiO₂ dielectric layer thermally grown on the highly doped p-type Si substrate. EBL (JEOL 6510 with Nanometer Pattern Generation System (NPGS)) was first employed to define the bottom electrode. The 100 nm thick ITO was achieved by magnetron sputtering (JSD300-III Magnetron) at a temperature of 100 °C as the top electrode. The image in figure 1(c) was obtained by a Bruker Multimode 8 with Scan Assist-Air probe under the peak force mode in ambient condition. The electrical and optoelectronic characterization were performed in ambient condition at room temperature using a Lake Shore probe station. The photoresponse to laser excitation measurements employed a focused laser beam ($\lambda = 637 \text{nm}$) from a Single Mode Fiber-Pigtailed LP637-SF70.

3. Results and discussion

3.1. Device structure and electrical characterization of MoS₂

Figure 1(a) shows the illustrative device schematic of the fabricated photodetector with vertical Schottky junctions of Au-MoS₂-ITO, while figure 1(b) displays the corresponding top-view optical microscope image of the device. It is clear that the device is constructed with multilayer MoS₂ sandwiched between the top ITO electrode and the bottom Au electrode pre-deposited on a highly p-doped Si/SiO₂ substrate, in which the composition and crystallinity of MoS₂ can be identified with Raman spectroscopy (supporting information figure S1 is available online at stacks.iop.org/NANO/28/484002/mmedia) [13]. Further investigation by atomic force microscope as displayed in figure 1(c) confirms that the device channel is 90 nm in the thickness, being the multilayer MoS₂. During the device fabrication, electron-beam lithography (EBL) is first used to define the bottom electrode, followed by the deposition of bottom electrode (Cr/Au, 15/50 nm). After the lift-off process, the multilayer MoS₂ is transferred on top of the bottom Cr/Au electrode. The

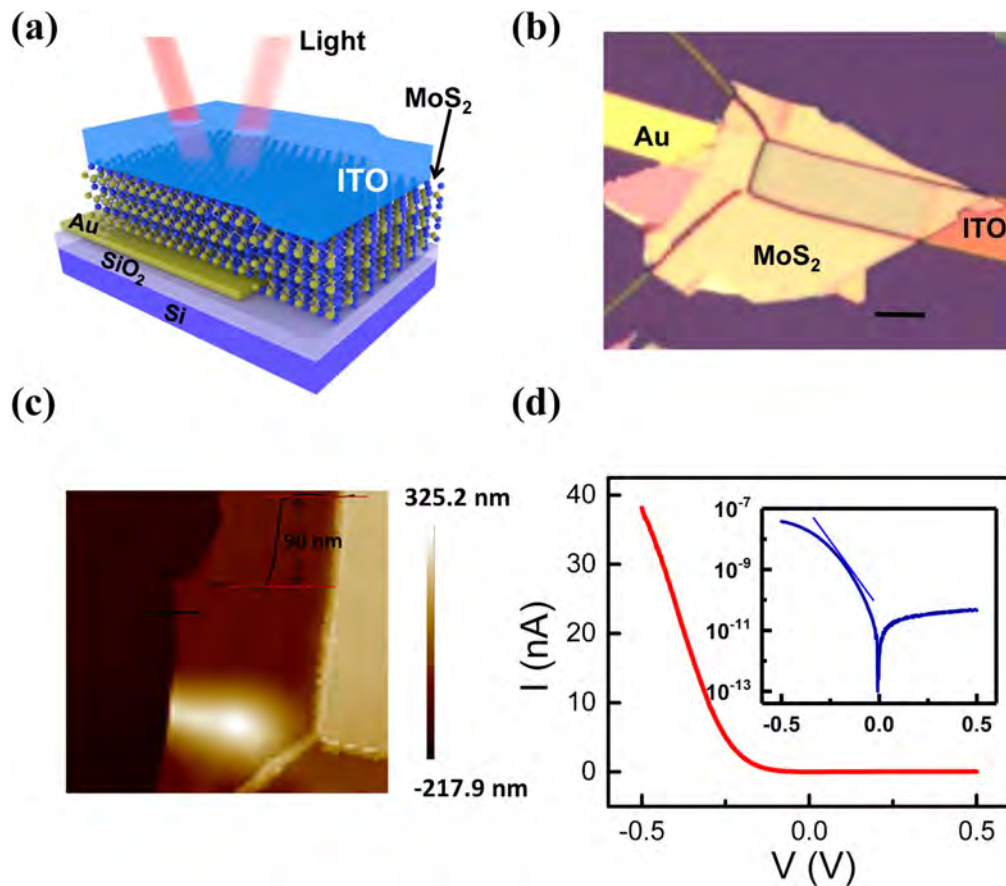


Figure 1. (a) Three-dimensional schematic view of the fabricated device. (b) The typical optical image of the device. The scale bar is $10\ \mu\text{m}$. (c) The AFM image of the multilayer MoS_2 transferred onto the substrate with the height profile measured for the deposited film thickness. (d) I - V characteristics of the fabricated photodetector measured in the dark at room temperature. The inset gives the same I - V curve in the logarithmic plot, showing remarkable rectifying I - V characteristics.

mechanical transfer process of MoS_2 onto the device substrate is performed within a glove box as described in supporting information figure S2. The top electrode of 100 nm thick ITO is then deposited by magnetron sputtering at a temperature of 375 K. The transmission spectrum of the deposited ITO film is as well depicted in supporting information figure S3, which demonstrates an acceptable transmittance (above 80%) ranging from 500 to 1000 nm. Importantly, figure 1(d) shows the I - V characteristics of the photodetector measured in dark at room temperature. The diode-like behavior with a considerable current rectification (i.e. forward/reverse current ratio, $I_F/I_R > 10^3$ at $|V| = 0.5\ \text{V}$) demonstrates that there exists a decent Schottky barrier. Since an ultralow reverse dark current of $\sim 10^{-12}\ \text{A}$ is achieved at zero bias voltage here, it can significantly improve the detectivity by distinguishing the photocurrent from the dark current. In addition, the I - V characteristics can be fitted well with an ideal diode equation of $I = I_s (e^{qV/nkT} - 1)$, where I is the diode current, I_s is the reverse saturation current, V is the voltage bias, q is the electron charge, k is the Boltzmann constant, T is the temperature and n is the ideality factor of the diode. By fitting the experimental data, an ideality factor of 2.1 is obtained, which is slightly higher than the ideal value of 2, suggesting few impurities at the interface or in the multilayer MoS_2 channel, even though these impurities are often observed in many

photoelectric materials [14]. The figure 1(d) inset also displays the logarithmic plot of I - V characteristics of the device, revealing the importance of contact barriers established between electrodes and MoS_2 for suppressing the dark current of the photodetectors achieved in this work.

To shed light on the operation mechanism of the vertical Schottky junction based photodetector, simplified energy band diagrams are employed to describe the photocurrent generation process taken place in dark and under illumination as depicted in figure 2. In general, for the Schottky-barrier structure, there are three distinct operational states, which are known as the equilibrium condition (i.e. $V = 0$), forward bias condition (i.e. $V > 0$) and reverse bias condition (i.e. $V < 0$). These three states can be independently activated with a suitable bias voltage such that the surface barrier defined at the MoS_2/Au interface can be precisely modulated. Explicitly, figure 2(a) illustrates the equilibrium energy band diagram of the fabricated Schottky-barrier structure with a stack of $\text{Au-MoS}_2\text{-ITO}$ at $V = 0$. Because the work function of Au metal (5.1 eV) is higher than that of the MoS_2 (4.6 eV), the electrons in MoS_2 would be injected into the Au electrode in order to maintain the equilibrium of Fermi energy when they are contacted with each other. This way, an ideal built-in electric field of 0.5 eV could be formed in principle which can reduce the dark current at zero bias voltage [15]. Moreover, in

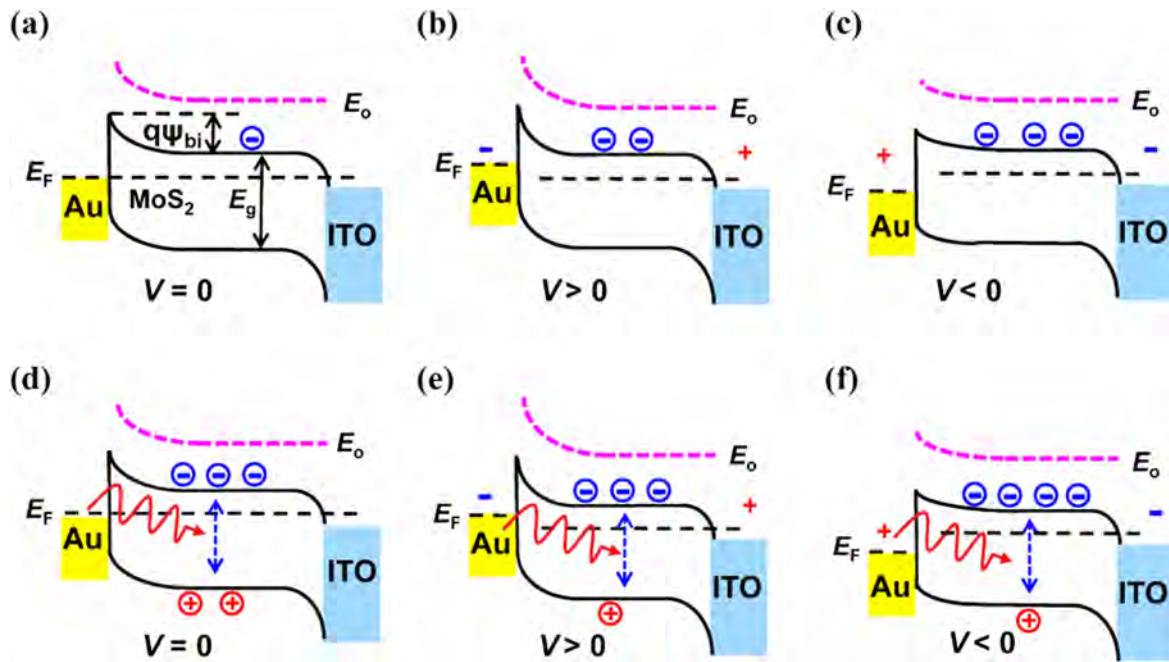


Figure 2. Simplified energy band diagrams at three distinct operation states with different bias voltage in dark (a)–(c) and under illuminations (d)–(f) to describe the corresponding photocurrent generation process. E_F is the Fermi level and $q\psi_{bi}$ represents the surface barrier. E_g and E_0 are the band gap of MoS₂ and vacuum level, respectively.

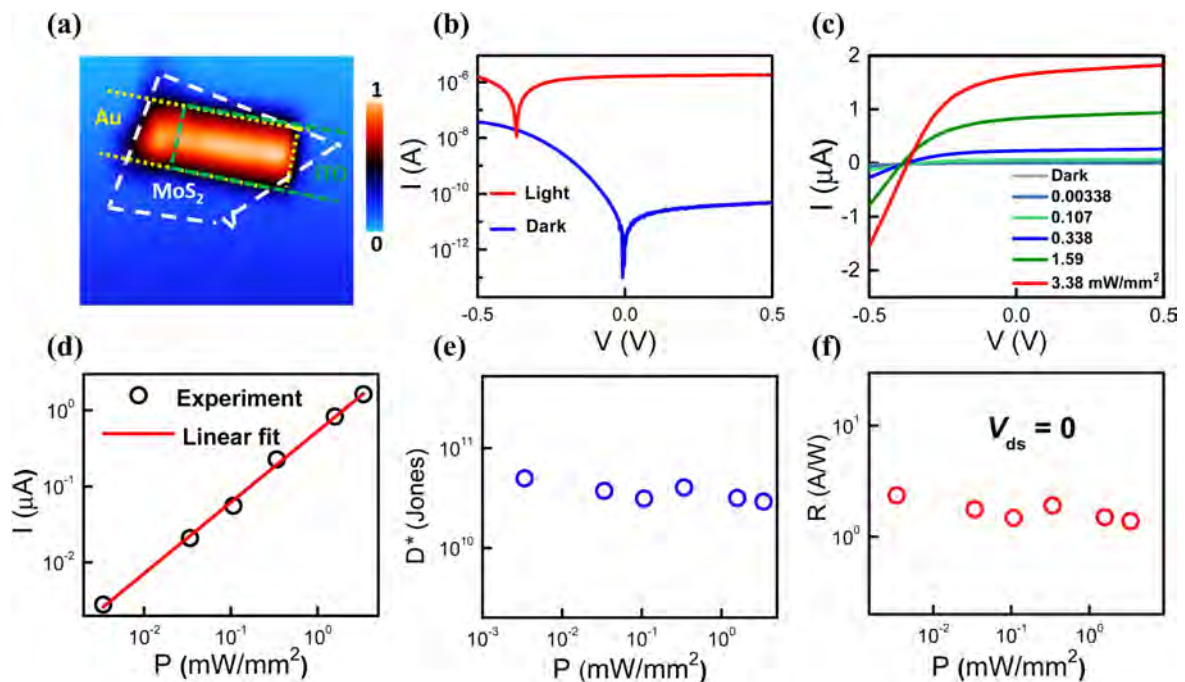


Figure 3. (a) The white, yellow and green lines represent the location of MoS₂ channel, Au and ITO electrodes, respectively. The photocurrent mapping of the device reveals prominent photocurrent generation between Au and MoS₂. (b) Output characteristics of the device in dark and under illumination with a power density of 3.38 mW mm⁻². The blue and red lines represent the dark current and the photocurrent, respectively. (c) Output characteristics of the device under different illumination power intensities. (d) The incident power dependence of the device photocurrent. (e) and (f) The incident power dependence of the device R and D^* , accordingly.

this particular device configuration, the reflected light coming from the bottom Au electrode can further enhance the detectivity of the photodetector. On the other hand, the top ITO electrode employed is a heavily doped (n-type)

transparent conductive oxide with a relative low work function of 4.5 eV; therefore, this ITO would form an almost perfect Ohmic contact with the intrinsically n-type MoS₂ channel. Notably, the above discussion ignores the influences

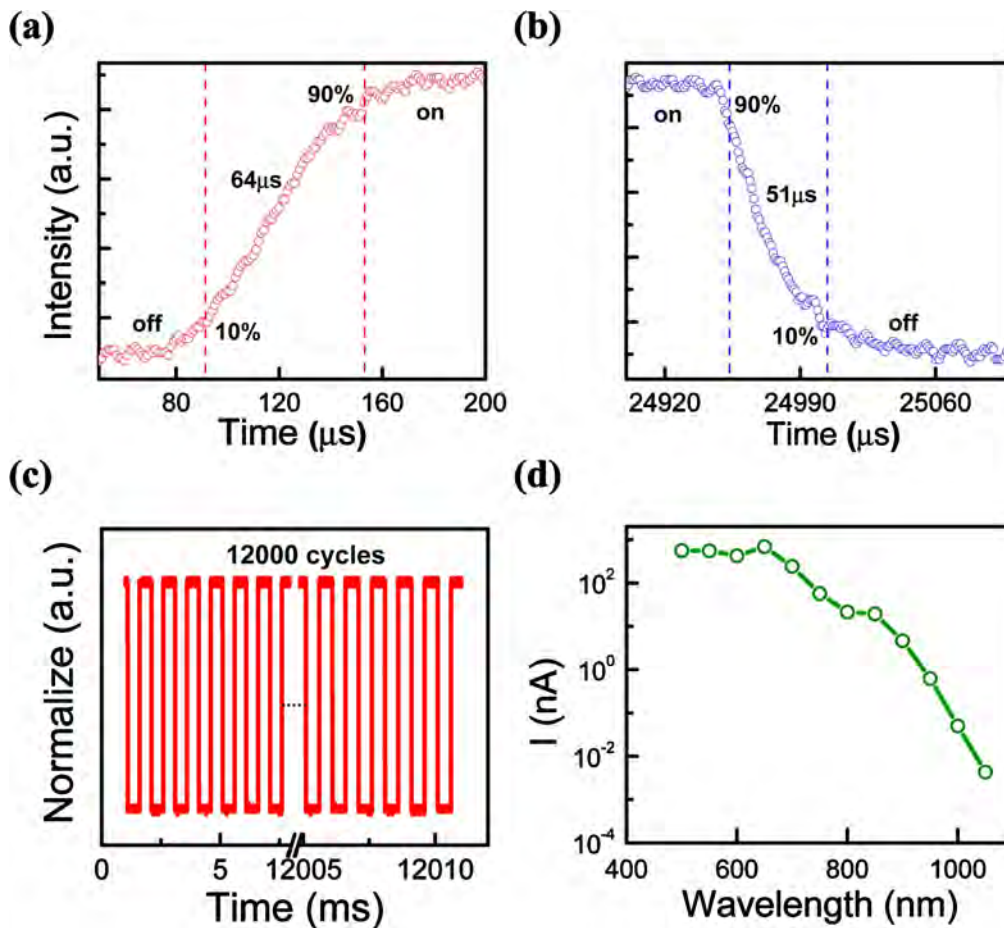


Figure 4. (a) and (b) present the rising and decaying edge of the detector at $V = 0$ with a laser of 637 nm. The time constants of 64 μs and 51 μs are obtained, respectively. (c) Stability test of the device. During 12 000 cycles of the switching operation, the photocurrent and dark current of the device remain unchanged. (d) The photocurrent measured as a function of the incident photon with the wavelength.

of any interface state, which may lead to Fermi level pinning and reduce effective work function of both Au and ITO [16]. Also, as compared with the forward and reverse bias conditions, there exhibits the lowest dark current in this equilibrium state due to the large surface barrier. Under illumination, the electrons in the valence band of MoS₂ are excited into the conduction band and separated near or in the depletion region owing to the built-in electric field, which forms an effective photovoltage driving the external circuit. The ultralow dark current can then be ignored as compared with the relatively large photocurrent as shown in figure 2(d). Meanwhile, the photocurrent at the forward bias (figure 2(e)) can be even larger than that of the equilibrium state (figure 2(d)) due to the steep downward energy band bending near Au/MoS₂ interface, which accelerates the separation of the electron-hole pairs at $V > 0$ within the breakdown voltage. In contrary, as shown in figure 2(c), the surface barrier is manipulated to be much smaller at $V < 0$, resulting in the larger thermionic current and thus decreasing the detectivity of the device [17, 18]. Therefore, the vertical Schottky junction is confirmed to play a crucial role in the photodetection studied in this work, in which this barrier can be modulated precisely by the bias voltage for different operation modes of the detector.

3.2. Performance evaluation of the MoS₂ photodetector

In order to verify the above mentioned photodetecting mechanism, the photocurrent generation of the device can be mapped by scanning photocurrent microscopy at $V = 0$, where a focused laser beam is scanned over the entire device and the corresponding photocurrent at each microscopic location is then extracted, as shown in figure 3(a). It is obvious that the spatially resolved photocurrent map reveals prominent photocurrent generation in the overlapping region between Au and MoS₂ stacked in the vertical manner, while there is almost no photocurrent generation in the other regions. All these imply that there is an effective Schottky-barrier established between Au and MoS₂ whereas an Ohmic contact between ITO and MoS₂, which is consistent with the analysis concluded in figure 2. Furthermore, corresponding output characteristics of the device under the 637 nm laser illumination is presented in figure 3(b). An impressively high photocurrent to dark current ratio of $I_{\text{light}}/I_{\text{dark}} \approx 10^6$ is obtained at a power density of 3.38 mW mm^{-2} , suggesting an excellent sensitivity to the incident light for the detector. Also, the output characteristics and photocurrent of the device are measured with different illumination power intensity (figures 3(c) and (d)). With increasing light intensity, more

free electrons are generated and then driven by the built-in potential, which is independent of the illumination power (if the illumination power is enough), forming larger photocurrents at zero voltage bias. However, when the voltage bias is precisely offset against the open circuit voltage, the photo-induced carriers are unable to establish an effective flow and then contribute to an insignificant current.

At the same time, responsivity (R) and specific detectivity (D^*) are two critical parameters employed to evaluate the sensitivity of detectors. R is given by I_p/P , where I_p designates the photocurrent in the detector and P represents the power density of illumination. Assuming that shot noise is the major factor contributing to the dark current, the detectivity can be expressed as $D^* = RA^{1/2}/(2eI)^{1/2}$ [19, 20], where R is the responsivity, A is the area of the photodetector and I is the dark current. As demonstrated in figures 3(e) and (f), the responsivity (R) and detectivity (D^*) of the photodetector are found to be $\sim 1 \text{ A W}^{-1}$ and $\sim 10^{10}$ Jones, respectively, under various illumination power densities ranging from 0.00338 all the way to 3.38 mW mm^{-2} at $V = 0$, indicating that the vertical junction based device is extremely sensitive to the incident illumination.

Moreover, the temporal photoresponse is another crucial performance parameter for photodetectors, determining the capability of distinguishing a fast signal. To study the response speed, a high-speed digital oscilloscope was used to record the current following the high-frequency modulated laser. Figures 4(a) and (b) show one entire cycle of the time-resolved photoresponse with both rising and decaying edges at an illumination density of 3.38 mW mm^{-2} ($\lambda = 637 \text{ nm}$). The rise time (t_{rise}) and decay time (t_{decay}) of photodetector is defined as the total time required for the output to rise from 10% to 90% of the pulse peak and to fall from 90% to 10%, respectively. The rising and decaying edges can also be perfectly fitted by single exponential functions, which yield the time constants of 64 and 51 μs for our detectors, being much faster than other MoS_2 based detectors reported in the literature [10–12]. This superb fast photoresponse can be ascribed to two reasons: (1) the shorter channel length configured in the vertical direction can substantially decrease the carrier transit time. (2) The built-in electric field can further accelerate the photogenerated electron–hole pair separation. Furthermore, the signals recorded by the oscilloscope do not exhibit any noticeable change after 12 000 cycles of operation as depicted in figure 4(c), indicating the excellent stability and reliability of the photodetector. Besides, based on the band gap of multilayer MoS_2 (i.e. 1.2 eV) [20–22], the fabricated device should be able to detect photons with the wavelength up to 1030 nm, which is longer than one of 850 nm corresponding to the indirect bandgap transition [12, 23]. Indeed, as shown in figure 4(d), the vertical Schottky junction based detector studied here displays a decent photocurrent and responsivity with the wavelength ranging from visible to 1000 nm (the responsivity as function of the wavelength is shown in figure S6). Such wide spectrum photoresponse can as well be attributed to the low dark current of 10^{-12} A and the shorter channel length for the efficient extraction of photocurrent, in addition to the relatively small bandgap of

multilayer MoS_2 channel. All these results clearly present an effective route to achieve the excellent and comprehensive optoelectronic performance for vertical Schottky-barrier photodetectors based on 2D materials.

4. Conclusion

In summary, a simple MoS_2 based photodetector utilizing vertical Schottky junctions of Au- MoS_2 -ITO is demonstrated. This simple unique device structure can enable the excellent photodetector performance, including an ultralow dark current of 10^{-12} A and a superb fast photoresponse of $\sim 64 \mu\text{s}$ at zero bias voltage. The responsivity and detectivity can also reach $\sim 1 \text{ A W}^{-1}$ and $\sim 10^{10}$ Jones, respectively. Importantly, the detection spectrum is superior to most recently reported pure MoS_2 photodetectors. These detectors can exhibit a wide detection spectrum with the wavelength ranging from visible to near-infrared (i.e. 0.7–1 μm), revealing its potential applications in optoelectronic devices. All these results indicate clearly the technological potency of multilayer MoS_2 configured in vertical Schottky junctions with Au electrode for the development of high-performance photodetectors.

Acknowledgments

The authors thank James Torley from the University of Colorado at Colorado Springs for critical reading of the manuscript. This work was partially supported by the State Key Program for Basic Research of China (2014CB921600), Natural Science Foundation of China (Grant Nos. 11734016, 61674157, and 61521005), and Key research project of frontier science of CAS (Grant Nos. QYZDB-SSW-JSC031).

Author Contributions

FG and HF contributed equally to this work. WH and JW conceived and supervised the research. FG fabricated the devices. FG and HF performed the measurements. WH, JW, FG and HF wrote the paper. All authors discussed the results and revised the manuscript.

ORCID iDs

Johnny C Ho  <https://orcid.org/0000-0003-3000-8794>

Weida Hu  <https://orcid.org/0000-0001-5278-8969>

References

- [1] Xia F N, Mueller T, Lin Y M, Valdes-Garcia A and Avouris P 2009 Ultrafast graphene photodetector *Nat. Nanotechnol.* **4** 839–43

- [2] Mak K F, Lee C, Hone J, Shan J and Heinz T F 2010 Atomically thin MoS₂: A new direct-gap semiconductor *Phys. Rev. Lett.* **105** 136805
- [3] Lee C, Yan H, Brus L E, Heinz T F, Hone J and Ryu S 2010 Anomalous lattice vibrations of single- and few-layer MoS₂ *ACS Nano* **4** 2695–700
- [4] Ganatra R and Zhang Q 2014 Few-layer MoS₂: a promising layered semiconductor *ACS Nano* **8** 4074–99
- [5] Bertolazzi S, Brivio J and Kis A 2011 Stretching and breaking of ultrathin MoS₂ *ACS Nano* **5** 9703–9
- [6] Das S, Chen H Y, Penumatcha A V and Appenzeller J 2013 High performance multilayer MoS₂ transistors with scandium contacts *Nano Lett.* **13** 100–5
- [7] Yin Z Y, Li H, Li H, Jiang L, Shi Y M, Sun Y H, Lu G, Zhang Q, Chen X D and Zhang H 2012 Single-layer MoS₂ phototransistors *ACS Nano* **6** 74–80
- [8] Xia F N, Mueller T, Golizadeh-Mojarad R, Freitag M, Lin Y M, Tsang J, Perebeinos V and Avouris P 2009 Photocurrent imaging and efficient photon detection in a graphene transistor *Nano Lett.* **9** 1039–44
- [9] Lopez-Sanchez O, Lembke D, Kayci M, Radenovic A and Kis A 2013 Ultrasensitive photodetectors based on monolayer MoS₂ *Nat. Nanotechnol.* **8** 497–501
- [10] Gong F *et al* 2016 High-sensitivity floating-gate phototransistors based on WS₂ and MoS₂ *Adv. Funct. Mater.* **26** 6084–90
- [11] Yu W J, Liu Y, Zhou H L, Yin A X, Li Z, Huang Y and Duan X F 2013 Highly efficient gate-tunable photocurrent generation in vertical heterostructures of layered materials *Nat. Nanotechnol.* **8** 952–8
- [12] Wang X D *et al* 2015 Ultrasensitive and broadband MoS₂ photodetector driven by ferroelectrics *Adv. Mater.* **27** 6575
- [13] Li H, Zhang Q, Yap C C R, Tay B K, Edwin T H T, Olivier A and Baillargeat D 2012 From bulk to monolayer MoS₂: evolution of Raman scattering *Adv. Funct. Mater.* **22** 1385–90
- [14] Barote M A, Yadav A A, Chavan T V and Masumdar E U 2011 Characterization and photoelectrochemical properties of chemical bath deposited N-Pbs thin films *Dig. J. Nanomater. Bios.* **6** 979–90
- [15] Das S, Prakash A, Salazar R and Appenzeller J 2014 Toward low-power electronics: tunneling phenomena in transition metal dichalcogenides *ACS Nano* **8** 1681–9
- [16] Kaushik N, Nipane A, Basheer F, Dubey S, Grover S, Deshmukh M M and Lodha S 2014 Schottky barrier heights for Au and Pd contacts to MoS₂ *Appl. Phys. Lett.* **105** 113505
- [17] Mouafo L D N, Godel F, Froehlicher G, Berciaud S, Doudin B, Kamalakar M V and Dayen J F 2017 Tuning contact transport mechanisms in bilayer MoSe₂ transistors up to Fowler–Nordheim regime *2d Mater.* **4** 01537
- [18] Wang P *et al* 2017 Arrayed Van Der Waals broadband detectors for dual-band detection *Adv. Mater.* **29** 1604439
- [19] Konstantatos G and Sargent E H 2010 Nanostructured materials for photon detection *Nat. Nanotechnol.* **5** 391–400
- [20] Wang J L, Fang H H, Wang X D, Chen X S, Lu W and Hu W D 2017 Recent progress on localized field enhanced two-dimensional material photodetectors from ultraviolet-visible to infrared *Small* **13** 1700894
- [21] Frey G L, Elani S, Homyonfer M, Feldman Y and Tenne R 1998 Optical-absorption spectra of inorganic fullerene-like MS₂ (M = Mo, W) *Phys. Rev. B* **57** 6666–71
- [22] Wang J L and Hu W D 2017 Recent progress on integrating two-dimensional materials with ferroelectrics for memory devices and photodetectors *Chin. Phys. B* **26** 037106
- [23] Choi W *et al* 2012 High-detectivity multilayer MoS₂ phototransistors with spectral response from ultraviolet to infrared *Adv. Mater.* **24** 5832–6